Dynamic Jahn-Teller Effect in the NV^- Center in Diamond

Tesfaye A. Abtew,[1] Y. Y. Sun,[2] Bi-Ching Shih,[1] Pratibha Dev,[1] S. B. Zhang,[2] and Peihong Zhang[1]
[1]*Department of Physics, University at Buffalo, State University of New York, Buffalo, New York 14260, USA*
[2]*Department of Physics, Applied Physics, and Astronomy, Rensselaer Polytechnic Institute, Troy, New York 12180, USA*
(Received 26 May 2011; published 30 September 2011)

The negatively charged nitrogen-vacancy (NV^-) center in diamond is considered to be one of the most promising solid state systems for quantum information applications. Excited states of the NV^- center play a center role in the proposed applications. Using a combination of first-principles calculations and vibronic interaction model analysis, we establish the presence of a dynamic Jahn-Teller effect in the ^3E excited state. The calculated temperature-dependent dephasing rate for the zero phonon line as well as the splitting of the first two vibronic states are in good agreement with experiment.

DOI: 10.1103/PhysRevLett.107.146403 PACS numbers: 71.70.Ej, 31.15.A−, 71.55.−i, 81.05.ug

A nitrogen-vacancy (NV) center in diamond is formed by an N substitution and a nearest neighbor vacancy, which can capture an extra electron to form an NV^-. The NV^- centers in diamond, with their unique spin and optical properties, have emerged as a promising solid system for studying spin-related phenomena [1]. The local spin states of the NV^- center can be accessed and manipulated optically at a single-site level [2], making it suitable for quantum information applications [3–8]. The ground state of the NV^- center in diamond is a spin triplet with an electronic configuration $(a_1^2e^2)[^3A_2]$ as shown in Fig. 1. The electron in the minority spin a_1 state can be optically excited to the unoccupied e state, forming a spin triplet excited state ^3E with a zero phonon excitation energy of 1.945 eV [9]. The excited state is orbitally degenerate and should experience either static or dynamic Jahn-Teller (JT) effects [10]. More precisely, the orbitally degenerate electronic state (E) will couple with a doubly degenerate (e) vibrational mode, resulting in an $E \otimes e$ JT system.

The dynamics of the excited state will be strongly affected by the JT instability. For example, a recent measurement [11] of the temperature dependence of the optical transition linewidth and excited states population relaxation of a single NV^- center suggests that the dynamic JT effect is the dominant mechanism for the optical dephasing at low temperatures. In addition, both the spin-orbit interaction [12] and the system's response to external perturbations (e.g., electric field and stress) will be significantly reduced (known as vibronic reduction or the Ham effect [13]) in the presence of the JT vibronic coupling. Since the ^3E excited state plays a central role in the optical initialization and readout of the spin states [14] and in the use of the NV^- center as a single photon source [3,15], it is very important to understand the JT effect in this system. Recently, using the local vibration modes of the NV^- center in diamond, possible consequences of the JT vibronic coupling on the optical adsorption process are discussed using symmetry analysis [16]. The stiff diamond lattice, however, makes the JT energy rather small. As a result, although the JT effect has been studied extensively for some impurity centers in oxides [17], it has been a challenge to study the JT effect in diamond [18]. Establishing the JT parameters is of critical importance for understanding the nature of the JT instability (i.e., static or dynamic) in this system. In this work, we use a quadratic $E \otimes e$ vibronic interaction model to analyze the numerical results obtained from first-principles calculations. We then calculate the dephasing rate for the zero phonon line (ZPL) as well as the splitting of the first two vibronic states. Our results compare well with experiment.

Within the quadratic $E \otimes e$ JT vibronic model [19], the splitting of the doubly degenerate electronic state under the influence of an e-type distortion is governed by the Hamiltonian

$$H^{\mathrm{el}}(Q_x, Q_y) = E_0 + \frac{K}{2}(Q_x^2 + Q_y^2)\sigma_z + F(Q_x\sigma_z - Q_y\sigma_x) + G[(Q_x^2 - Q_y^2)\sigma_z + 2Q_xQ_y\sigma_x)], \quad (1)$$

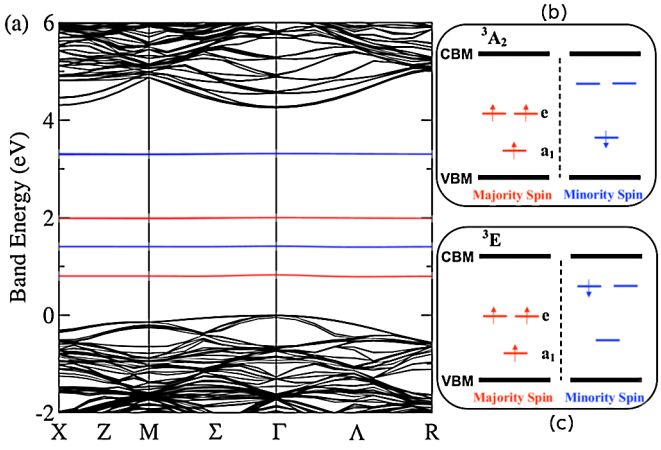

FIG. 1 (color online). (a) Band structure of the ground state of the NV^- center in diamond. (b) Schematic one electron energy levels of the ground state ($^3A_2$). (c) Schematic one electron energy levels of the excited state (^3E).

where σ_x and σ_z are Pauli matrices, E_0 is the energy of the degenerate electronic state at $Q_x = Q_y = 0$, Q_x and Q_y are the displacement vectors from the C_{3v} structure as shown in Fig. 2(a). The three vibronic constants are K, the elastic force constant, F, the linear vibronic constant, and G, the quadratic vibronic constant. In polar coordinates with $\rho = \sqrt{(Q_x^2 + Q_y^2)}$ and $\phi = \arctan(Q_y/Q_x)$, the solution for Eq. (1) yields two sheets of the adiabatic potential energy surface (APES) [19],

$$\epsilon(\rho, \phi) = \tfrac{1}{2}K\rho^2 \pm \rho[F^2 + G^2\rho^2 + 2FG\rho\cos(3\phi)]^{1/2}. \quad (2)$$

If the quadratic coupling $G = 0$, the lower sheet of the APES has the form of a surface of revolution often called the "Mexican hat." For a nonzero quadratic coupling ($G \neq 0$), three minima develop along the trough of the Mexican hat with a displacement ρ_0 as shown in Fig. 2(b). These energy minima have an energy that is E_{JT} lower than the undistorted structure and are separated by an energy barrier δ.

In order to obtain the numerical parameters in the quadratic $E \otimes e$ vibronic model, we carry out density functional theory (DFT) [20,21] based first-principles electronic structure calculations using the QUANTUM ESPRESSO [22] package. The generalized gradient approximation of Perdew, Burke, and Ernzerhof [23] is used for the exchange and correlation terms. Electron-ion interactions are described by ultrasoft pseudopotentials [24]. The plane wave basis has an energy cutoff of 50 Ry to ensure the convergence of the calculations.

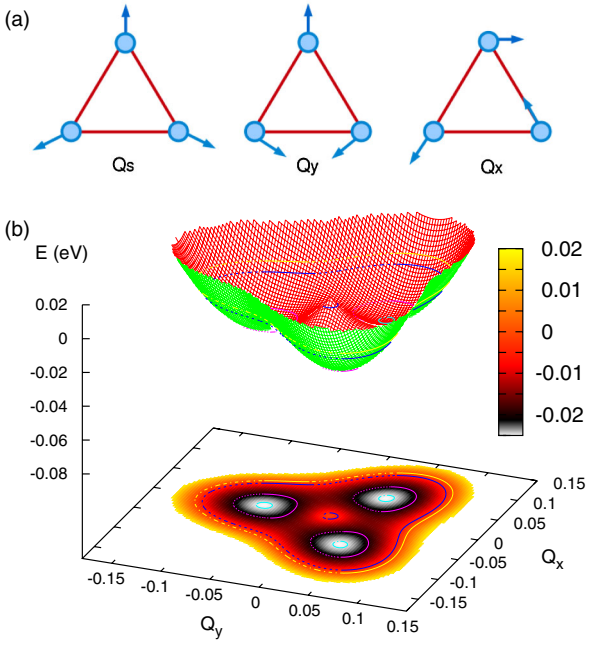

FIG. 2 (color online). (a) Three normal modes of a structure with the C_{3v} symmetry: totally symmetric displacement mode, Q_s (a_1 type) and degenerate Q_x and Q_y modes (e type). (b) The adiabatic potential energy surface for the NV^- center in diamond.

The electronic structure calculations for the NV^- center are carried out using a 512-atom supercell structure. We first perform a structural relaxation to obtain the ground state structure. Substantial local relaxation is observed. For example, the volume of the tetrahedron formed by the substitutional nitrogen and three carbon surrounding the vacancy expands by about 20% due to the broken bonds around the vacancy and the formation of shorter N-C bonds (1.47 Å). The C-C bonds near the vacancy site shrink by about 3% compared with the ideal value. As mentioned earlier, the ground state of the NV^- center has a C_{3v} symmetry with an electronic configuration $(a_1^2 e^2)[^3A_2]$. The calculated spin-resolved band structure [Fig. 1(a)] shows the nearly dispersionless in-gap one electron defect states (a_1 and e), indicating that the interaction between periodic images of the defect is negligible.

The excited state ^3E is obtained by a spin conserving excitation of an electron from $a_1^{\downarrow}$ to $e^{\downarrow}$ as shown schematically in Fig. 1(c). As mentioned above, the orbitally degenerate excited state will couple with the e-type local vibration modes (LVM) Q_x and Q_y [Fig. 2(a)], giving rise to a classic $E \otimes e$ JT system [19]. The first step towards characterizing the JT effect is to calculate the APES [19] for the excited state. This is done by carrying out constrained DFT calculations. Figure 2(b) shows the calculated APES for the excited state; the APES is plotted with respect to the two orthogonal e-type displacement modes Q_x and Q_y. Three equivalent local minima are found near the C_{3v} symmetric point with a JT stabilization energy ($E_{\mathrm{JT}} = E_{\mathrm{min}} - E_{C_{3v}}$) of 25 meV. The local minima are separated by an energy barrier δ of 10 meV. In these lower energy configurations, atoms near the defect center distort significantly from their positions in the C_{3v} configuration. The three carbon atoms near the vacancy (labeled C_1, C_2, and C_3) form an equilateral triangle in the undistorted structure, which becomes an obtuse isosceles triangle in the distorted structure. The C_1-C_2, C_2-C_3, and C_3-C_1 distances are changed by -0.72%, $+0.85\%$, and -0.72%, respectively, relative to the undistorted carbon-carbon distances.

It should be pointed out that the distortion to the ideal structure with a C_{3v} symmetry is not limited to the three carbon atoms near the vacancy site. The distortion is a collective displacement of all atoms involved in the e-type LVM with the Q_x (or Q_y) symmetry. Figure 3 shows the displacement vector associated with one of the local minima, which clearly shows the Q_y symmetry of distortion.

With these first-principles results at hand, we now analyze the JT effects in this system in more details. First, the JT parameters ρ_0 (the distortion magnitude), E_{JT} (the JT stabilization energy), and δ (the barrier between local minima) are related to the vibronic coupling constants defined in Eq. (1) as follows: $\rho_0 = F/(K - 2G)$,

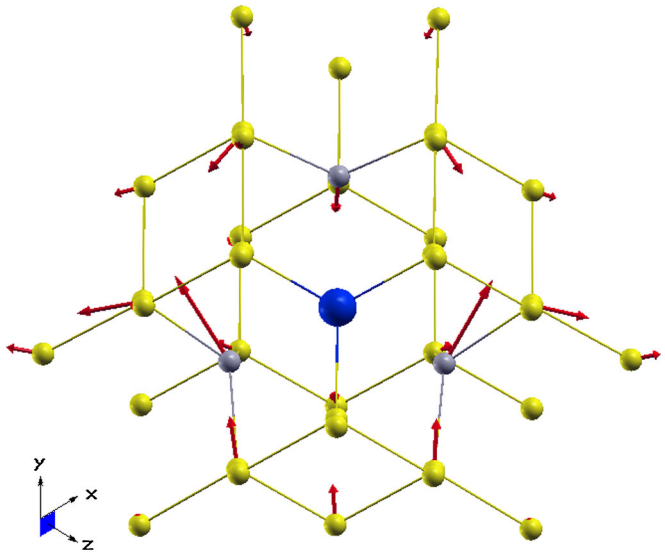

FIG. 3 (color online). Displacement vector associated with one of the local minima. Only atoms near the NV center are shown for clarity. Gray (small sphere) is for the carbons near the vacancy, yellow (light small sphere) is for the other carbons, and blue (big sphere) is for nitrogen.

$E_{\mathrm{JT}} = F^2/2(K - 2G)$, and $\delta = 4E_{\mathrm{JT}}G/(K + 2G)$. Using the parameters obtained from first-principles calculations ($\rho_0 = 0.068$ Å, $E_{\mathrm{JT}} = 25$ meV, and $\delta = 10$ meV), we find the corresponding vibronic coupling constants $F = -0.74$ eV/Å, $G = 1.76$ eV/Å^2, and $K = 14.5$ eV/Å^2.

Before we can proceed further to discuss the dynamical aspect of the ^3E excited state, we need to evaluate another important quantity, namely, the phonon energy of the LVM involved. Unfortunately, it is not practical to calculate the energy of the LVM of a JT system directly using standard phonon calculation techniques. This is because the system is intrinsically unstable at the degenerate point. We can, however, estimate this phonon energy using the diagonal quadratic constant K mentioned above, which gives an energy ($\hbar\omega$) for the LVM of 71 meV. This energy is also very close to the energy (65 meV) of the same LVM of the ground state.

Although an exact solution to the coupled vibronic problem is still out of reach, with these results at hand, we can now make a few observations regarding the nature of the JT effect in this system. First, the vibronic coupling in this system is weak (but not very weak) as measured by the dimensionless coupling constant $\lambda = E_{\mathrm{JT}}/\hbar\omega = 0.35$. [The coupling is considered to be weak if $\lambda \ll 1$ (strong if $\lambda \gg 1$) [19].] Second, since the shallow energy minima are separated by an energy barrier (10 meV) that is much smaller than the phonon energy, $\hbar\omega = 71$ meV, the vibrational states (even the ground state) of the system cannot be localized in one of the minima. If we neglect the quadratic coupling constant G, the low vibrational states of the system involve radial vibration and free rotation of the distorted configuration along the bottom of the trough of the Mexican hat potential well. In the presence of the quadratic coupling G, however, this internal rotation is hindered.

An important parameter for understanding the dynamics of a JT system is the so-called tunneling splitting (called 3Γ in the case of $E \otimes e$ JT system) [25]. The idea is that, insofar as the lowest vibronic states are concerned, the local vibrational wave functions associated with the three energy minima in the lower sheet of the APES [Fig. 2(b)] can be used as the zeroth-order wave functions for subsequent perturbation treatments. The tunneling between the local minima results in a splitting (3Γ) between the vibronic E-type and A-type states. If the system has deep energy minima that are separated by a high energy barrier (i.e., $\delta \geq \hbar\omega$), the tunneling effect is weak and the system can be regarded as being trapped in the one of the local minima with occasional tunneling between minima. The tunnel rate is related to the tunneling splitting 3Γ.

However, as discussed above, the energy barrier ($\delta \sim 10$ meV) in this system is small. Strictly speaking, the concept of occasional tunneling between localized vibration states is not valid here. The dynamics of the ground state of the system is better described by a hindered internal rotation. Nevertheless, we can still use the energy separation between the lowest energy (E-type) vibronic state and the first excited state (A-type) as a measure of the degree of the localization (or delocalization) of the vibrational states. In order to obtain the full vibronic spectrum, we diagonalize the vibronic Hamiltonian

$$H^{\mathrm{JT}} = H^{\mathrm{el}}(Q_x, Q_y) - (\hbar^2/2M)(\partial^2/\partial Q_x^2 + \partial^2/\partial Q_y^2) \quad (3)$$

within the subspace spanned by the electronic doublet and the vibrational states of the simple harmonic oscillator of the unperturbed system, i.e., $\Psi_{j,n_x,n_y} = \phi_j(\vec{r})\chi_{n_x}(Q_x)\times\chi_{n_y}(Q_y)$. Here ϕ_j ($j = 1, 2$) is the electronic wave function and χ_{n_x} (χ_{n_y}) is the vibrational wave function associated with the Q_x (Q_y) LVM. The Hamiltonian is diagonalized with the vibrational quantum numbers n_x and n_y up to 20. The results for the lowest few vibronic states are shown in Table I. The splitting between the E-type vibronic ground state and the A-type first excited state is 35 meV. This is significantly larger than the energy barrier (10 meV) between the energy minima, indicating that this is a dynamic JT system. It is interesting to mention that the vibronic ground state of the coupled (distorted) system has the same E symmetry as the ground state of the undistorted system (i.e., the reference system at $\vec{Q} = 0$). Table I also lists the lowest few vibronic levels calculated without including the quadratic coupling (i.e., with $G = 0$). Note that in the absence of the quadratic coupling, the vibronic states with the A_1 and A_2 symmetry are accidentally degenerate, as it was shown by Longuet-Higgins *et al.* [26].

Finally, we discuss a few important and experimentally measurable consequences of the JT effects in this system.

TABLE I. Calculated vibronic levels.

Symmetry	Energy ($G \neq 0$) (meV)	Energy ($G = 0$) (meV)
E	36.7	39.3
A_1	71.7	91.0
A_2	103.8	91.0
E	114.8	127.8
E	143.7	146.6
A_1	166.1	197.6
E	183.7	192.8
A_2	199.6	197.6

As mentioned earlier, a recent measurement [11] clearly suggested that the dephasing of the ZPL of the NV^- center at low temperatures is dominated by the coupling between the electronic E doublet and the e phonons. The measured T^5 dependence of the linewidth of the ZPL was explained by a two-phonon Raman process (i.e., a second-order perturbation treatment of a linear JT Hamiltonian), which results in a dephasing rate [see also Eq. (2) of Fu *et al.* [11]]

$$W = \frac{2\pi}{\hbar}\int_0^{\hbar\omega_D} dE n(n+1)\rho^2(E)\frac{V^4(E)}{E^2}, \qquad (4)$$

where $E = \hbar\omega$ is the phonon energy, n is the phonon occupation number, ρ is the phonon density of states (DOS) associated with the e_x or the e_y phonon, $V(E)$ is the linear coupling constant, and $\hbar\omega_D$ is an appropriate cutoff energy (the Debye energy) for this problem. The coupling constant $V(E)$ defined here is related to the linear coupling constant F defined earlier through $V = F\sqrt{\hbar/2M\omega}$, where M is the mass of the carbon atom. Note that the Debye energy used here must not be confused with those defined in other contexts. Using the Debye model for the phonon DOS and assuming that the coupling constant scales as $\sqrt{E}$ [11], i.e., $V(E) = C\sqrt{E}$, the above integral can be simplified

$$W = \frac{8\pi}{\hbar}\left(\frac{\Omega}{2\pi^2\hbar^3 v_s^3}\right)^2 C^4 (k_B T)^5 I_4\left(\frac{\hbar\omega_D}{k_B T}\right), \qquad (5)$$

where $I_4(\frac{\hbar\omega_D}{k_B T}) = \int_0^{\hbar\omega_D/k_B T} dx[x^4 e^x/(e^x-1)^2]$ is the Debye integral, $v_s = 1.2\times 10^4$ m/s is the sound velocity in diamond, Ω is the volume of the diamond unit cell. We use the calculated coupling constant $F = 0.74$ eV/Å at $\hbar\omega_0 \approx 70$ meV to obtain the coupling constant C through $C\sqrt{\hbar\omega_0} = F\sqrt{\hbar/2M\omega_0}$. At the low temperature limit, the Debye integral $I_4(\infty) = 4\pi^4/25$. Finally, we have, for the low temperature limit, $W = 38.2T^5(\mathrm{s}^{-1})$. This compares surprisingly well with the experimental result $W = 0.5c_2 rT^5 = (36.8 \pm 2.0)T^5(\mathrm{s}^{-1})$ [11]. Using an appropriate cutoff energy, we can calculate the full temperature-dependent dephasing rate. Figure 4 compares the measured and the calculated temperature-dependent linewidth

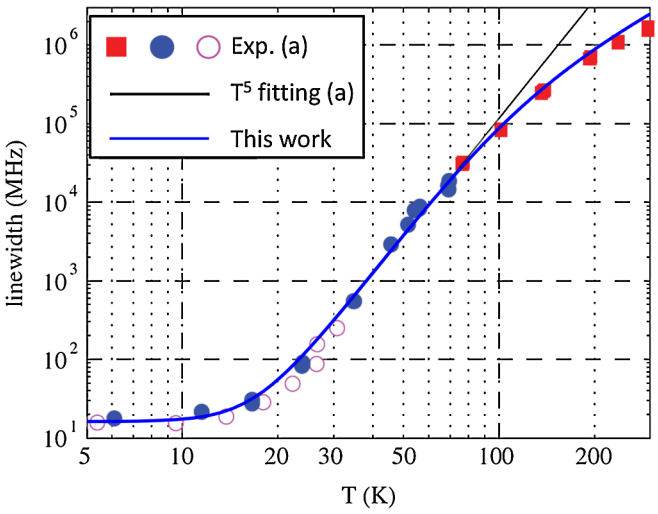

FIG. 4 (color online). Comparison between the calculated and the measured linewidth of the ZPL of the NV^- center in diamond. (a) Experimental results and the T^5 fitting are taken from Ref. [11].

$\gamma(T) = \gamma_0 + 2W(T)$ (rescaled by a factor of $1/2\pi$) using $\hbar\omega_D = 50$ meV and $\gamma_0 = 2\pi\times 16.2$ MHz taken from Ref. [11].

Another experimental signature of the JT effect is the splitting of the first vibrational peak of the absorption spectra of the NV^- center [9]. The calculated splitting of the first two bright vibronic excited states (A_2 and E) is 11 meV (Table I), this is very close to the experimental value of about 10 meV [9]. The position of the first vibration peak is about 60 meV from the ZPL [9], which again agrees well with the calculated value of 67 meV. The transition to the A_2 state is allowed for photon polarization parallel to the symmetry axis whereas for the perpendicular polarization, transitions to E states are allowed. We caution that our model cannot reproduce faithfully results for higher vibronic states since coupling to other phonon modes (e.g., a_1) will greatly modify high vibronic states.

In conclusion, we use a quadratic $E \otimes e$ vibronic model to understand the JT effect in the ^3E excited state of the NV^- center in diamond. The vibronic coupling parameters are obtained from DFT-based first-principles electronic structure calculations. Diagonalization of the coupled vibronic Hamiltonian gives the vibronic spectrum with a splitting (3Γ) between the vibronic ground state and the first excited state of about 35 meV, resulting in a barrier to tunneling splitting ratio, $\delta/3\Gamma$, of 0.29. Our results indicate that the ^3E excited state of the NV^- center in diamond is a dynamic JT system. The computed dephasing rate for the ZPL as well as the splitting of the first two vibronic states agree well with experiment.

We thank Elif Ertekin and Jeffrey C. Grossman for helpful discussion during the course of this work. We acknowledge the computational support provided by the

Center for Computational Research at the University at Buffalo, SUNY. This work is supported by the Department of Energy under Grant No. DE-SC0002623.

[1] D. Awschalom, R. Epstein, and R. Hanson, Sci. Am. **297**, 84 (2007).
[2] A. Gruber *et al.*, Science **276**, 2012 (1997).
[3] A. Beveratos *et al.*, Phys. Rev. Lett. **89**, 187901 (2002).
[4] L. Childress *et al.*, Science **314**, 281 (2006).
[5] M. G. Dutt *et al.*, Science **316**, 1312 (2007).
[6] G. Balasubramanian *et al.*, Nature Mater. **8**, 383 (2009).
[7] J. R. Maze *et al.*, Nature (London) **455**, 644 (2008).
[8] G. D. Fuchs *et al.*, Nature Phys. **6**, 668 (2010).
[9] G. Davies and M. F. Hamer, Proc. R. Soc. A **348**, 285 (1976).
[10] H. A. Jahn and E. Teller, Proc. R. Soc. A **161**, 220 (1937).
[11] K.-M. C. Fu *et al.*, Phys. Rev. Lett. **103**, 256404 (2009).
[12] I. B. Bersuker and B. G. Vekhter, Sov. Phys. Solid State **5**, 1772 (1964).
[13] F. S. Ham, in *Electron Paramagnetic Resonance*, edited by S. Geschwind (Plenium, New York, 1972).
[14] F. Jelezko, T. Gaebel, I. Popa, A. Gruber, and J. Wrachtrup, Phys. Rev. Lett. **92**, 076401 (2004).
[15] C. Kurtsiefer, S. Mayer, P. Zarda, and H. Weinfurter, Phys. Rev. Lett. **85**, 290 (2000).
[16] A. Gali, T. Simon, and J. E. Lowther, New J. Phys. **13**, 025016 (2011).
[17] P. Garcia-Fernandez, A. Trueba, M. T. Barriuso, J. A. Aramburu, and M. Moreno, Phys. Rev. Lett. **104**, 035901 (2010).
[18] G. Davies, J. Phys. C **12**, 2551 (1979).
[19] I. B. Bersuker, *The Jahn-Teller Effect* (Cambridge University Press, Cambridge, U.K., 2006).
[20] P. Hohenberg and W. Kohn, Phys. Rev. **136**, B864 (1964).
[21] W. Kohn and L. J. Sham, Phys. Rev. **140**, A1133 (1965).
[22] P. Giannozzi *et al.*, J. Phys. Condens. Matter **21**, 395502 (2009).
[23] J. P. Perdew, K. Burke, and M. Ernzerhof, Phys. Rev. Lett. **77**, 3865 (1996).
[24] D. Vanderbilt, Phys. Rev. B **41**, 7892 (1990).
[25] I. B. Bersuker, Sov. Phys. JETP **16**, 933 (1963).
[26] H. C. Longuet-Higgins, U. Opik, M. H. L. Pryce, and R. A. Sack, Proc. R. Soc. A **244**, 1 (1958).